Supplemental Information

Materials and methods

Generation of transgenic human parkin overexpressing mice

To generate transgenic mice overexpressing human wildtype parkin (wt h-parkin) the open reading frame (ORF) of wild type parkin (1398 bp) was inserted downstream to the murine prion promoter in the phgMmPrP vector (60) by replacing exon 3 (ORF of PrPC) after SceI restriction digest. The final plasmid was digested with SalI and NotI to remove the bacterial backbone. The linearized vector was microinjected into the pronuclei of single cell embryos of the FvB/NJ mouse line. Offsprings were screened for the presence of the human transgene by PCR using a forward primer binding to exon 4 (h-parkin Tg Fwd, ACCTGCAGGCAGGCAACGCTCAC) and a reverse primer binding to exon 7 (h-parkin Tg Rev, GCAGGGAGTAGCCAAGTTGAGGG). Under the used PCR conditions the large intronic sequence of the endogenous murine parkin locus could not be amplified, whereas the human parkin ORF resulted in a 361bp DNA fragment. Two different founders were backcrossed with wildtype C57BL/6J mice for at least 10 generations.

Tissue lyses and sample preparation for Western blotting

For mouse tissue, dissected SN and striatum samples from control and mutant mice were homogenized using Dounce homogenizers in pre-cooled in lysis buffer containing 50 mM Tris HCl pH-7.5, 150 mM NaCl, 0.5% triton x-100 with appropriate amounts of protease and phosphatase inhibitor cocktail (Roche) using Teflon Dounce. The homogenate was centrifuged at 20000g for 15 min at 4˚C. For Triton X-100 insoluble fraction, supernatants were used for Western blotting. For Triton X-100 insoluble fraction, the pellets obtained after the 20000g centrifugation step were boiled in buffer containing 25 mM Tris pH 6.8, 1% SDS, 4% glycerol and 5% β-mercaptoethanol for 10 min at 95˚C, samples thus obtained were used for Western blotting.

For mammalian cell lines, cell pellets were lysed in 0.1% Triton X-100 in PBS with appropriate amounts of protease and phosphatase inhibitor cocktails (Roche) by pipetting up and down then centrifuged at 20000g for 15 min, supernatants were used for determining protein concentration using BCA followed by Western blotting.

Behavioral experiments

Open field: Male mice were placed for 10 min into a 50 x 50 cm arena enclosed by 40 cm high walls and their horizontal activity (total distance moved) and time spent in the border zone during the first 5 min was measured by a blinded investigator from the tracks recorded by the EthoVision software (Noldus) (61). The border zone was defined as the area less than 5 cm from the outer walls.

Pole test: Motor coordination is monitored in the 12 month old male mice while they are climbing down a vertical pole. The test is performed as already described (62). Mice are placed head upward on the top end of a rough-surfaced vertical wooden rod (60 cm long, 7 mm in diameter), under white light illumination (5-10 lux). To motivate the mouse, part of its nesting material/bedding is placed on the platform at the bottom of the pole. To test motor learning, each mouse is tested in three trials with an inter-trial interval of 30 sec during which the mouse is placed into its home cage. The time mice takes to reach the platform with all four paws and the manner by which they descended from the top of the pole (falling, climbing down after 180° rotation or turning of the body) is recorded. If a mouse stay at the top of the pole without apparently attempting to climb down, after 120 sec some nesting material from the mouse cage is handled immediately beneath the mouse so that it can smell it and hopefully try to climb down. The test is videotaped for analyzing the turning behavior, scores are given for turning (score = 100) and not turning (score = 0) behavior of each mouse in all the three trials, The 180° turning scores from all the three trials for each mice is quantified and represented in percentage.

Rotarod: Mice have to walk on a turning, corrugated rod (3.2 cm in diameter) (Accelerated Rotarod for mice, Jones & Roberts, TSE systems, Bad Homburg, Germany) under red light illumination. The rod is started 5 sec after the mice have been placed onto it. Mice undergo 5 trials with an inter trial interval of 45 min. Trials 1 and 2 are performed at slow, constant speed (4 rpm) for a maximum duration of 3 min. Trials 3-5 are performed with the accelerating rod, starting with 4 rpm up to 40 rpm within 4 min, with a maximum duration of 10 min. The performance of the mice is evaluated by scoring the average latency to fall (in sec), on an acellerating rotarod from the trials 3-5 (62).

Elevated plus maze: Male mice were placed in an elevated plus maze with four 30 cm long and 5 cm wide arms, connected by a 5 x 5 cm center. Two opposing arms were bordered by 15 cm high walls (closed arms), whereas the other two arms (open arms) were bordered by a 2

mm rim. The maze was elevated 75 cm from the floor and illuminated with 3 lux to allow video recording. The mouse was placed into the center facing one open arm and observed for 5 min. The following parameters were obtained from the pre-recorded video with the software The Observer (Noldus); entries and duration into the open arms (calculated when all four paws were on an open arm), entries into the end of the open arms (calculated when the mouse reaches with its snout the end of an open arm) and head dipping events (calculated when the mouse dips its head in the open arm) by a blinded investigator as previously described (63).

Astrocyte and microglial density quantifications

Every sixth section (30 μm thick coronal) from striatum and midbrain was used to determine the relative number of astrocytes (GFAP positive cells) or microglial cells (Iba1 positive cells) in the dorsal striatum and SNpc respectively. For each section, the area containing labeled cells was delineated and 3 images of dorsal striatum and 2 images of SN were acquired using the upright microscope Axio Imager.M1 (Zeiss, Goettingen, Germany). The number of cells was later determined from the images obtained from five sections per animal by using the cell counter plugin in the ImageJ program (NIH).

For morphological analysis of microglial cells in the SN region, a minimum of 100 cells from Iba1 antibody stained coronal midbrain sections from 24 months old mice across the genotypes are categorized as resting, bushy or amoeboid microglial cells based on their morphology as described (64). The analysis was performed using the cell counter plugin in the ImageJ program (NIH).

Electron microscopy study of mitochondria in DA cells

24 month old mice were perfused with 0.9% PBS and subsequently with fixative (4% paraformaldehyde and 0.1% glutaraldehyde). Brains were removed from the skulls and postfixed overnight in 4% paraformaldehyde at 4˚C. The brains were cut with a vibratome into 100 μm thick sections and incubated in 2.3 M sucrose (in PBS, pH 7.4) overnight at 4˚C. Sections were permeabilized by cracking, incubating the sections alternating in 2- methyl-butane (cooled below -100°C in liquid N2) and 2.3 M sucrose (at room temperature) for 3 min each for three times, washed three times with PBS for 5min each, incubated in 0.3% H_2O_2 for 5 min and washed with PBS. Sections were blocked with 0.3% BSA and 10% horse serum in 1X PBS for 30 min and then incubated with mouse anti-TH antibody (1:1000, Diasorin), diluted in carrier solution (1X PBS with 0.2% BSA and 1% horse serum) for 48 hrs at 4˚C.

After primary antibody incubation, sections were washed with PBS and incubated in HRP coupled anti-mouse secondary antibody (1:500, Vectastain) diluted in carrier solution for 2 hrs at room temperature and then washed with PBS before incubating the sections in Vectastain ABC solution (Vector Laboratories) for 2hrs at room temperature. The staining was performed after washing with 1X PBS with diaminobenzidine for 5 min followed by three 5 min washes with 1X PBS. The stained sections were rinsed three times in 0.1 M sodium cacodylate buffer (pH 7.2–7.4) and osmicated using 1% osmium tetroxide (Science Services) in cacodylate buffer. Following osmication, the sections were dehydrated using ascending ethyl alcohol concentration steps, followed by two rinses in propylene oxide. Infiltration of the embedding medium was performed by immersing the sections in a 1:1 mixture of propylene oxide and Epon and finally in neat Epon and hardened at 60 °C. Ultrathin sections (60nm) were examined on en electron microscope EM902 (Zeiss). Pictures were taken with a MegaViewIII digital camera (A. Tröndle).

Total number of mitochondria and percentage of damaged mitochondria per 100 μm^2 of cytosolic area was analyzed from 1500±250μm^2 TH immunolabeled cytosolic area of SNpc neurons per animal. Mitochondria were considered as damaged when the cristae were distorted or disrupted, when the outer membrane was detached or when the outer membrane had protrusions (32). For estimating the length of mitochondria, a minimum of 500 mitochondria were counted from 20–28 TH immunolabeled SNpc neurons per animal. We classified the mitochondria into two groups based on their length, smaller than 0.5µm and larger than 0.5µm, slightly different from what was described previously (29). The analysis was done independently by two examiners blinded to the genotype using the image J program (NIH).

Striatal total dopamine measurements

Dissected striatal tissue was homogenized in 0.1 M perchloric acid containing 0.5 mM disodium EDTA and 100 ng/ml, 3,4-dihydroxybenzylamine (internal standard) and then centrifuged at 50,000 g for 30 min. Pellets were resuspended in a neutralizing buffer for protein determination using BCA (Pierce); whereas, the supernatants after filtering through a 0.22 µM PVDF membrane were subjected to HPLC electrochemical detection system analysis as described previously(54) with 3,4 dihydrobenzylamine (100 ng/ml lysis buffer) as internal standard; flow rate of the mobile phase was 1.2 ml/min; the sample injection volume was 20 µl. The applied electrochemical potentials were: Conditioning cell = +10 mV; analytical cell:

E1 = + 50 mV; E2 = 360 mV. The retention times of the measured metabolites were as follows: DOPAC (3. 80 min), 3, 4-dihydroxybenzylamine (4.25 min), dopamine (6.88 min) and HVA (10.30 min). The peak areas of the metabolites were normalized with the peak area of the internal standard and values were represented as ng per mg of striatal protein.

Mitochondrial enrichment

Dissected SN tissue samples were homogenized in 1 ml and siRNA transfected cell pellets (obtained from one 6 well plate) were lysed in 0.5ml of pre-cooled homogenization buffer containing 320 mM sucrose, 5 mM Tris pH 7.4, 2 mM EGTA along with appropriate amounts of protease inhibitor cocktail (Roche). After ten strokes with a Teflon douncer (for tissue) or pipetting the pellet up and down for 30 times in the lysis buffer (for SH-SY5Y cells) the lysates were centrifuged for 3 min at 2000 g to remove nuclei and other cell particles. Supernatants were collected and centrifuged for 10 min at 12,000 g to pellet mitochondria and synaptosomes. The crude pellet was resuspended in 1 ml (for tissue) and 0.5 ml (for SH-SY5Y cells) of homogenization buffer containing 0.02% w/v of digitonin to disrupt synaptosomal membranes and release trapped mitochondria. The resuspended samples were centrifuged for 10 min at 12,000 g to pellet mitochondria, which were again resuspended in 100 µl of the homogenization buffer, and protein content was determined by BCA assay (Pierce).

Detection of protein oxidation

For detecting the carbonylation (oxidation) of proteins in control and mutant mice (24 months old), striatum and SN tissue sample lysates were prepared as described previously (4). After protein concentration determination using BCA (Pierce) assay, 15 µg of protein per sample was taken to detect protein carbonylation using Oxyblot kit (Millipore S7150), rest of the procedure was carried out according to the kit manufacturer's instructions.

Real-time RT-PCR

The following primers were used: Human (h) forward (F) primer parkin F 5'-AGTGTTTGTCAGGTTCAACTCCAGC-3', h parkin reverse (R) primer 5'-AACCCCCTGTCGCTTAGCAAC-3', h-Ret F 5'-CGGACATCAGCAAAGACC-3', h-Ret R

5'-GCCGTCGTCATAAATCAGG-3', h-β-actin F 5'-TGGACTTCGAGCAAGAGA-3', h-β-actin R 5'-AGGAAGGAAGGCTGGAAGAG-3'.

References

60. Fischer M, Rulicke T, Raeber A, Sailer A, Moser M, Oesch B, Brandner S, Aguzzi A, and Weissmann C. Prion protein (PrP) with amino-proximal deletions restoring susceptibility of PrP knockout mice to scrapie. *EMBO J.* 1996;15(6):1255-64.
61. Valenti P, Cozzio A, Nishida N, Wolfer DP, Sakaguchi S, and Lipp HP. Similar target, different effects: late-onset ataxia and spatial learning in prion protein-deficient mouse lines. *Neurogenetics.* 2001;3(4):173-84.
62. Freitag S, Schachner M, and Morellini F. Behavioral alterations in mice deficient for the extracellular matrix glycoprotein tenascin-R. *Behav Brain Res.* 2003;145(1-2):189-207.
63. Trullas R, and Skolnick P. Differences in fear motivated behaviors among inbred mouse strains. *Psychopharmacology (Berl).* 1993;111(3):323-31.
64. Gelderblom M, Melzer N, Schattling B, Gob E, Hicking G, Arunachalam P, Bittner S, Ufer F, Herrmann AM, Bernreuther C, et al. Transient receptor potential melastatin subfamily member 2 cation channel regulates detrimental immune cell invasion in ischemic stroke. *Stroke; a journal of cerebral circulation.* 2014;45(11):3395-402.

Supplemental Figure1

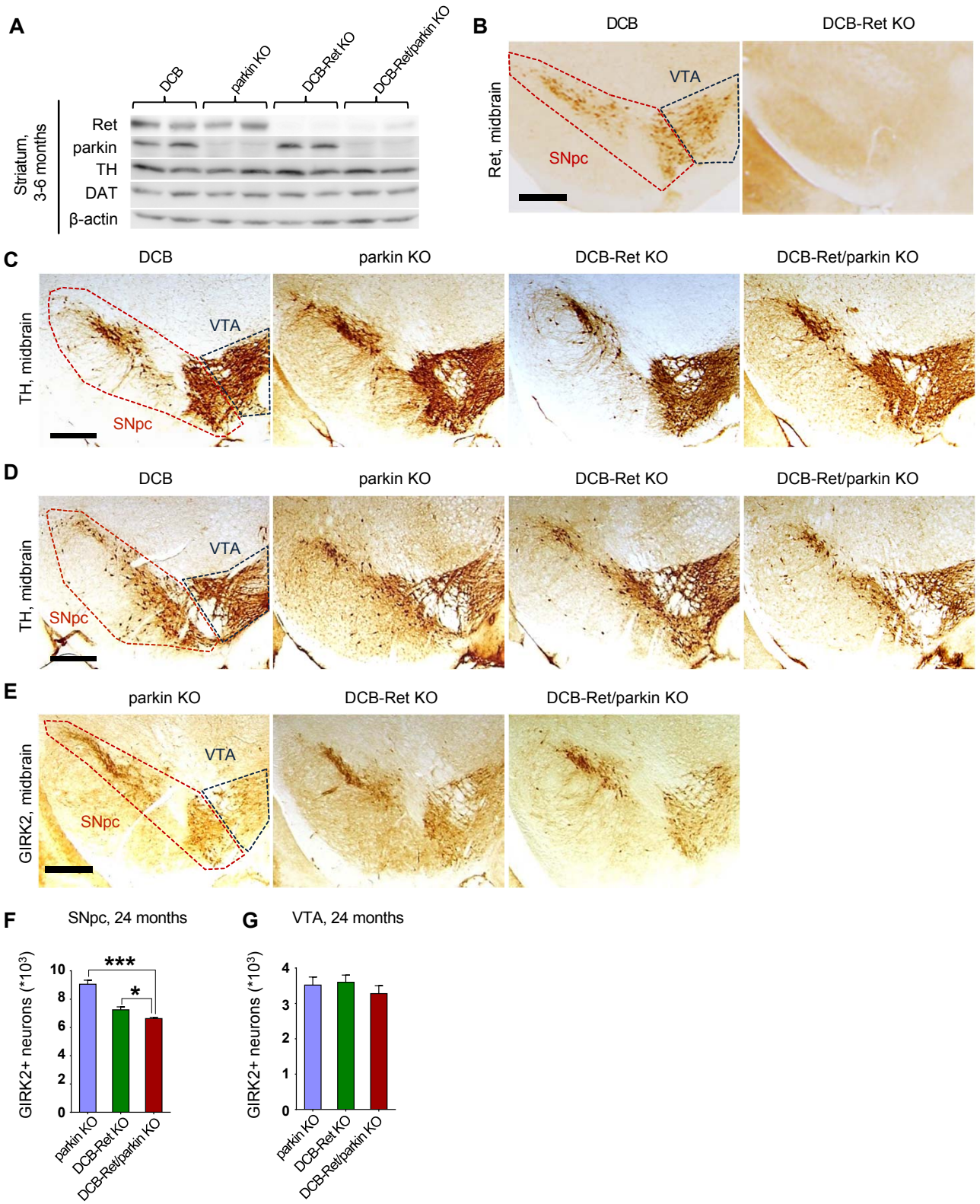

Supplemental Figure 1. Late-Onset and SN specific degeneration of DA neurons in mice lacking Ret and parkin. (**A**) Western blot analysis of Ret and parkin expression in striatal tissue lysates from 3 month old mice of the indicated genotypes confirmed the efficient deletion of parkin and Ret proteins in their respective knocKOuts without affecting TH and DAT protein levels, whereas β-actin is used as loading control. (**B**) Representative Ret immunostaining on coronal sections from DCB control and DCB-Ret KO mice confirmed the effective ablation of Ret protein both in the SN and VTA region. (**C and D**) Representative images of TH antibody stained DA neurons in the SNpc and VTA region in coronal sections from (C) 3-6 months and (D) 12 months old mice of the indicated genotypes (scale bar: 250 µm). (**E**) Representative images of GIRK2 expressing DA neurons in the SNpc and VTA in coronal sections from 24 months old mice of the indicated genotypes (scale bar: 250 µm). (**F and G**) Stereological quantifications of GIRK2 positive neurons in the (F) SNpc and (G) VTA of 24 months old mice of the indicated genotypes (n = 3-4).(data are represented as mean +/- SEM; * p≤0.05, *** p≤0.001; One-way ANOVA, Newman-Keuls post-hoc test).

Supplemental Figure 2

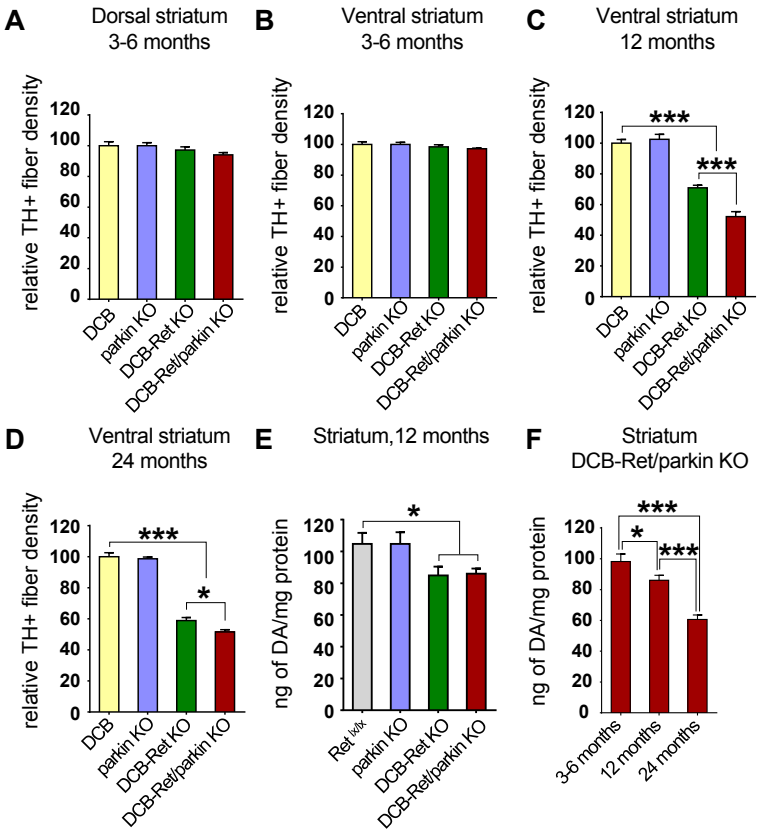

Supplemental Figure 2. Ret and parkin maintain DA innervation of the striatum. (**A to D**) Quantification of the TH fiber density in the (A) dorsal and (B) ventral striatum of 3-6 months, (C) ventral striatum of 12 months and (D) ventral striatum of 24 months old mice of the indicated genotypes (n = 3-4). (**E**) Total striatal dopamine levels in 12 months old mice of the indicated genotypes (n = 6-7). (**F**) Progressive and age dependent loss of total DA levels in the striatum of DCB-Ret/parkin KO (n=5-7) mice over time. Data are obtained from figure 4D, supplemental figure 2E and figure 2F (data are represented as mean +/- SEM; * p≤0.05, *** p≤0.001; One-way ANOVA, Newman-Keuls post-hoc test for A, B, C, D and F; unpaired two tailed t-test for E).

Supplemental Figure 3

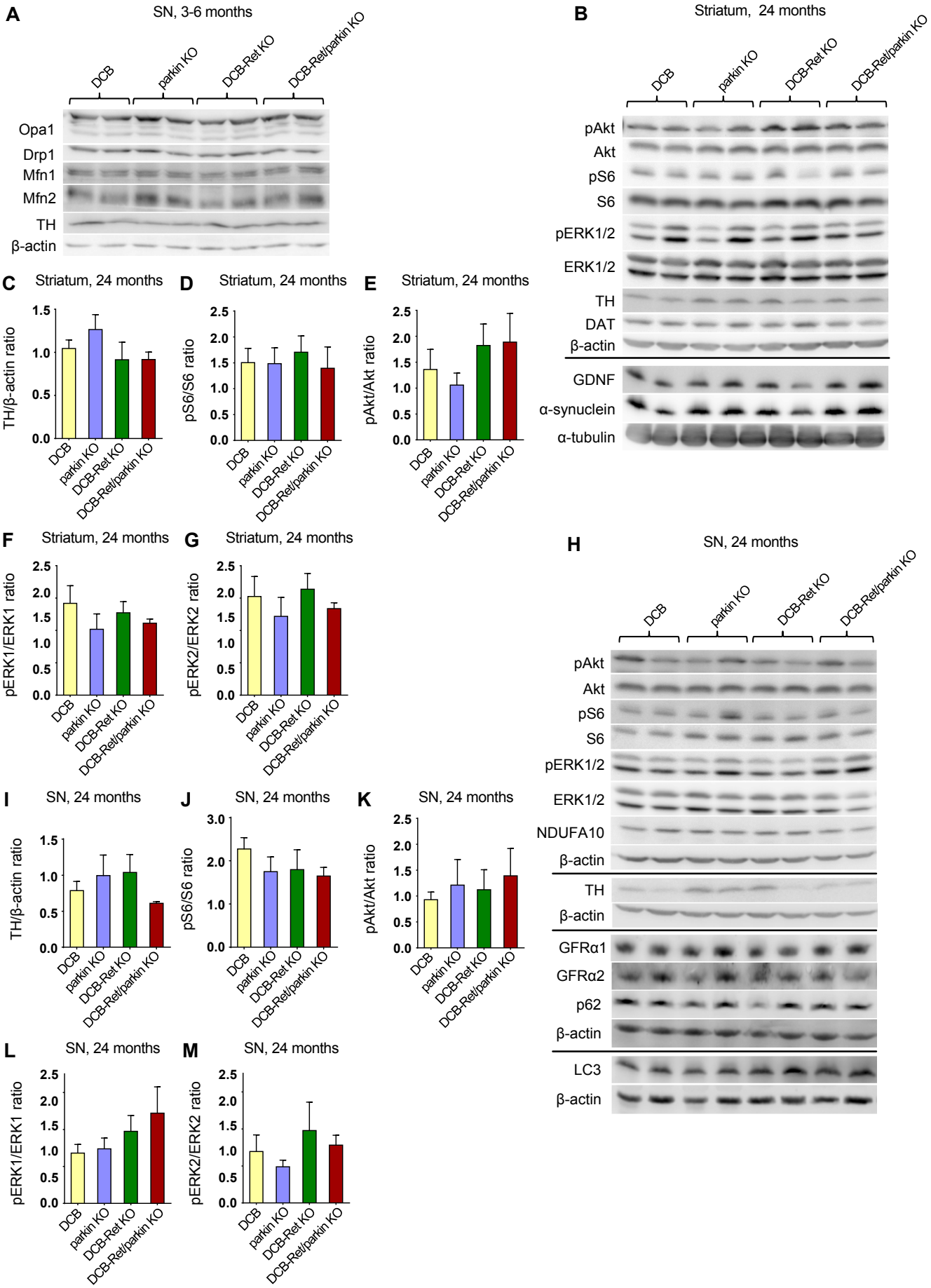

Supplemental Figure 3. Intracellular signaling changes in Ret/parkin-deficient mice. (**A**) Western blot images depicting expression of the indicated proteins in the SNpc of 3-6 months old mice; (**B**) Western blot images depicting expression of the indicated proteins in the striatum protein lysates of 24 months old mice and (**C - G**) Quantification of the relative ratio of (C) TH to β-actin, (D) phospho-S6 (pS6) to S6 (E) phospho-Akt (pAkt) to AKT, (F) phospho-ERK1 (pERK1) to ERK1 (G) phospho-ERK2 (pERK1) to ERK2 of indicated genotypes from the striatal lyates of 24 months old mice are shown (n = 4). (**H**) Western blot images depicting expression of the indicated proteins in the SNpc of 24 months old mice. (**I - M**) Quantification of the relative ratio of (I) TH to β-actin, (J) phospho-S6 (pS6) to S6 (K) phospho-Akt (pAkt) to AKT, (L) phospho-ERK1 (pERK1) to ERK1 (M) phospho-ERK2 (pERK1) to ERK2 of indicated genotypes from the SN lyates of 24 months old mice are shown (n = 4). Proteins probed on different blots are separated by horizontal lines in (B) and (H). β-actin or α-tubulin are shown as loading controls. (data are represented as mean +/- SEM; One-way ANOVA, Newman-Keuls post-hoc test).

Supplemental Figure 4

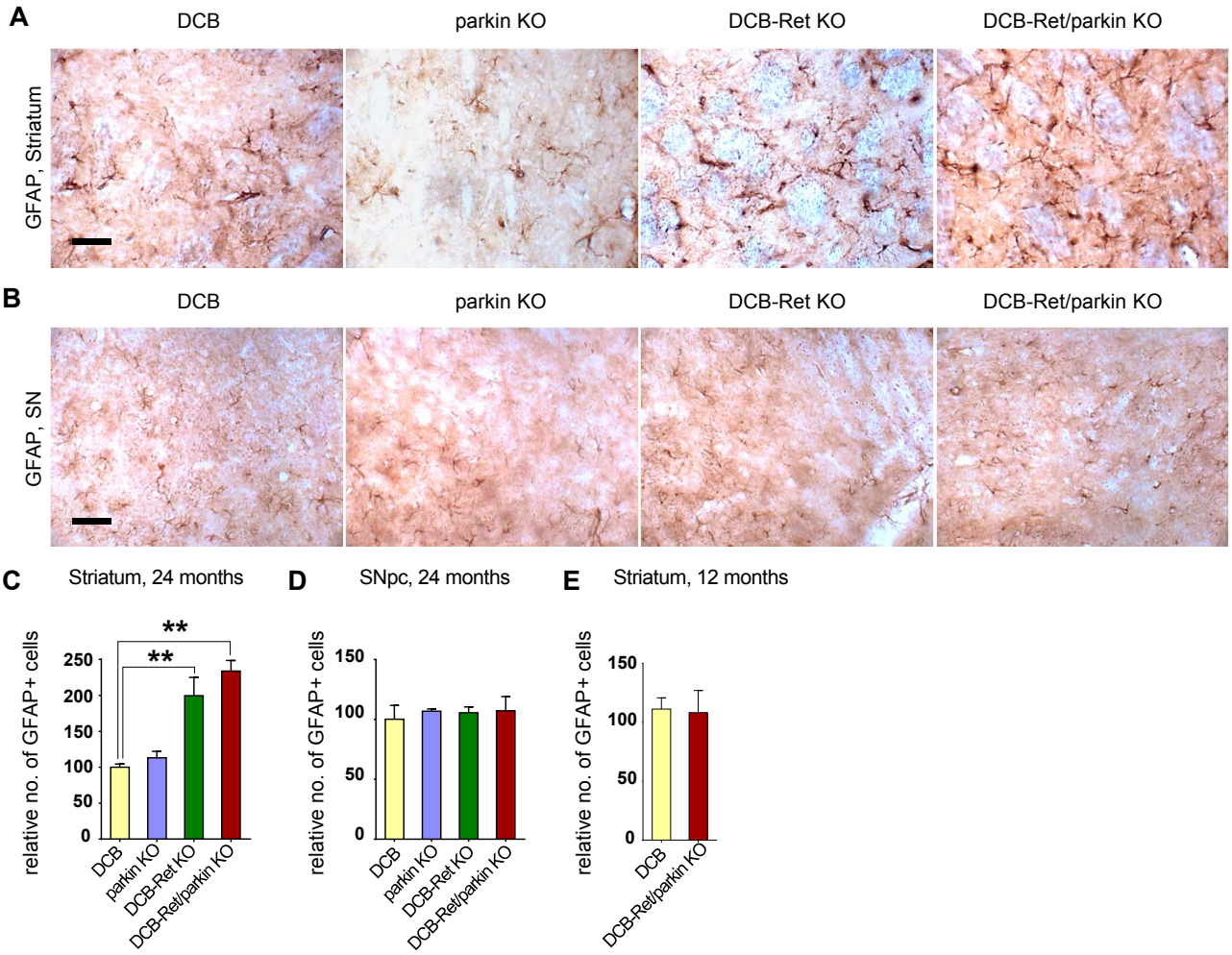

Supplemental Figure 4. Gliosis accompanies DA neuronal fiber degeneration in the striatum of aged Ret- and Ret/parkin- deficient mice. (**A and B**) Representative images of coronal sections from 24 months old mice of the indicated genotypes stained with glial fibrillary acidic protein (GFAP) antibody showing astrocytes in the (A) striatum and (B) SNpc (scale bar: 250 µm (**C – E**) Quantifications of GFAP positive cells in the (C) striatum of 24 months, (D) SNpc of 24 months and (E) striatum of 12 months old mice of the indicated genotypes (n = 3-4). (data are represented as mean +/- SEM; * p≤0.05, ** p≤0.01; One-way ANOVA, Newman-Keuls post-hoc test)

Supplemental Figure 5

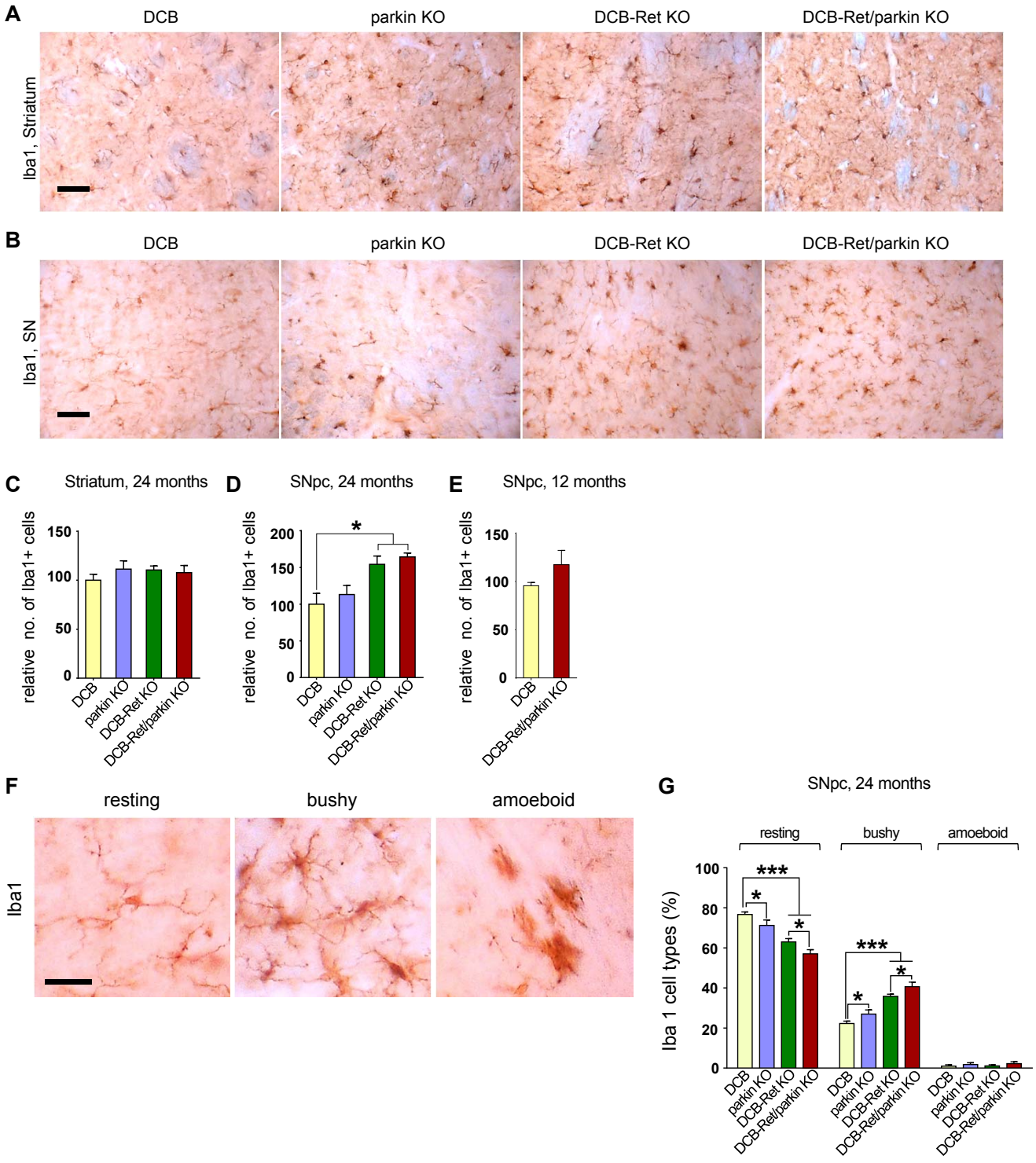

Supplemental Figure 5. Inflammation accompanies DA neuronal degeneration in the SNpc of aged Ret- and Ret/parkin- deficient mice. (**A and B**) Representative images of coronal sections from 24 months old mice of the indicated genotypes stained with ionized binding calcium adaptor molecule (Iba1) antibody showing microglia in the (A) striatum and (B) SNpc across the indicated genotypes (scale bar: 250 µm) (**C – E**) Quantifications of Iba1 positive cells in the (C) striatum of 24 months (D) SNpc of 24 months and (E) SNpc of 12 months old mice of the indicated genotypes (n = 3-4). (**F**) Representative images of resting, bushy and amoeboid microglial (Iba1) cell types in the SNpc of 24 months old mice (scale bar: 100 µm). (**G**) Quantifications of the resting, bushy and amoeboid microglial cell types in the SNpc of 24 months old mice across the indicated genotypes (n = 3). (data are represented as mean +/- SEM; * p≤0.05, *** p≤0.001; One-way ANOVA, Newman-Keuls post-hoc test for C and D; unpaired two tailed t-test for E; Two-way ANOVA, Newman-Keuls post-hoc test for G).

Supplemental Figure 6

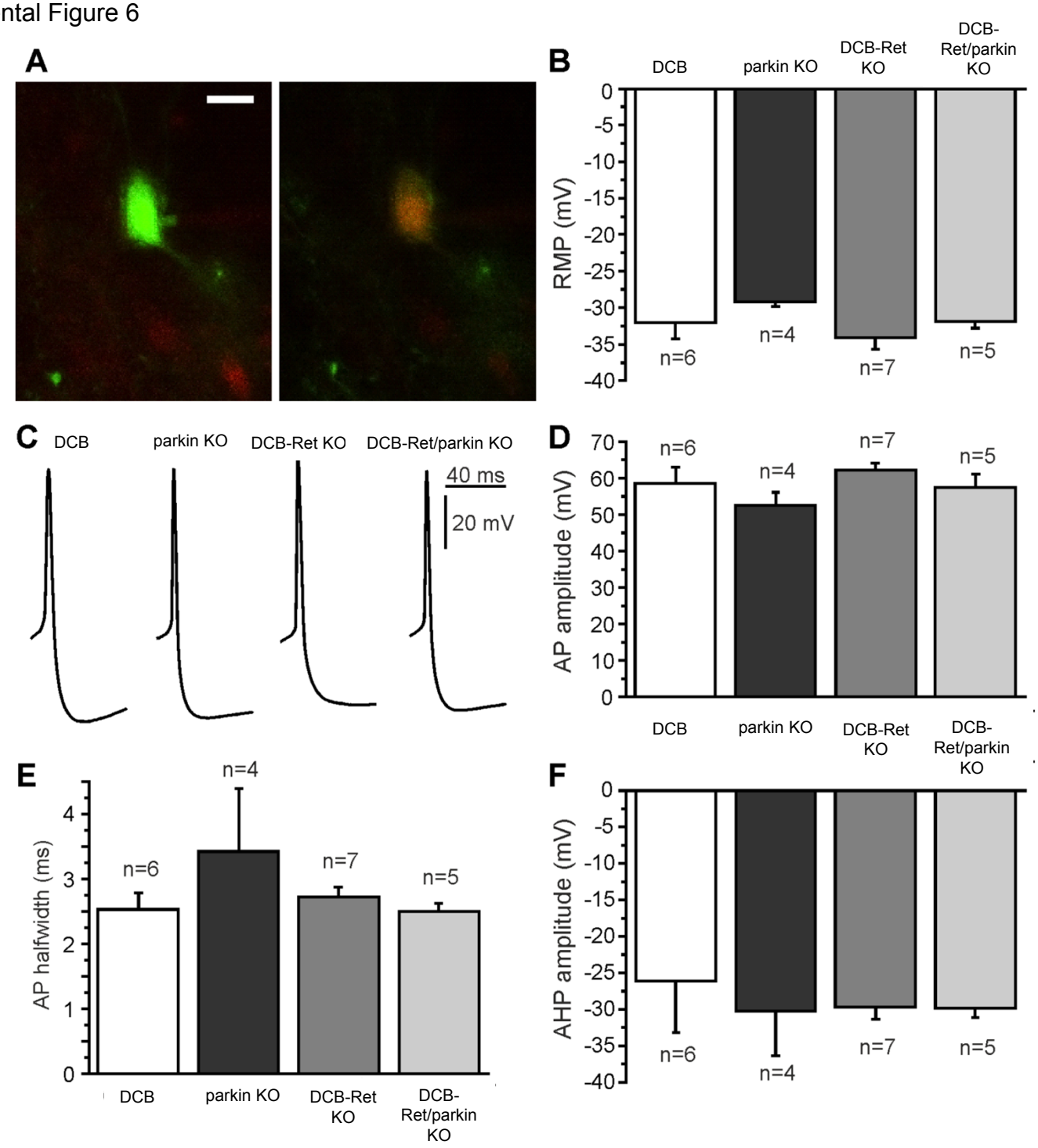

Supplemental Figure 6. Electrophysiological properties of SNpc DA neurons in adult mice. (A) A GFP-positive neuron (green, left panel) was targeted with an Alexa 594-filled patch pipette, resulting in orange-red staining of the cell upon successful establishment of the whole-cell configuration (right panel). Scale bar: 10 µm. (**B**) Resting membrane potential (RMP) of GFP-positive neurons in DCB, parkin KO, DCB-Ret KO and DCB-Ret/parkin KO mice. No significant differences in the resting membrane potential were found between the genotypes tested. (**C**) Action potentials measured in in DCB, parkin KO, DCB-Ret KO and DCB-Ret/parkin KO mice were very similar between genotypes. (**D-F**) No significant differences were found in the amplitude, the half width, nor in the amplitude of the action potentials after hyperpolarization between the genotypes tested. (data are represented as mean +/- SEM; One-way ANOVA, Newman-Keuls post-hoc test)

Supplemental Figure 7

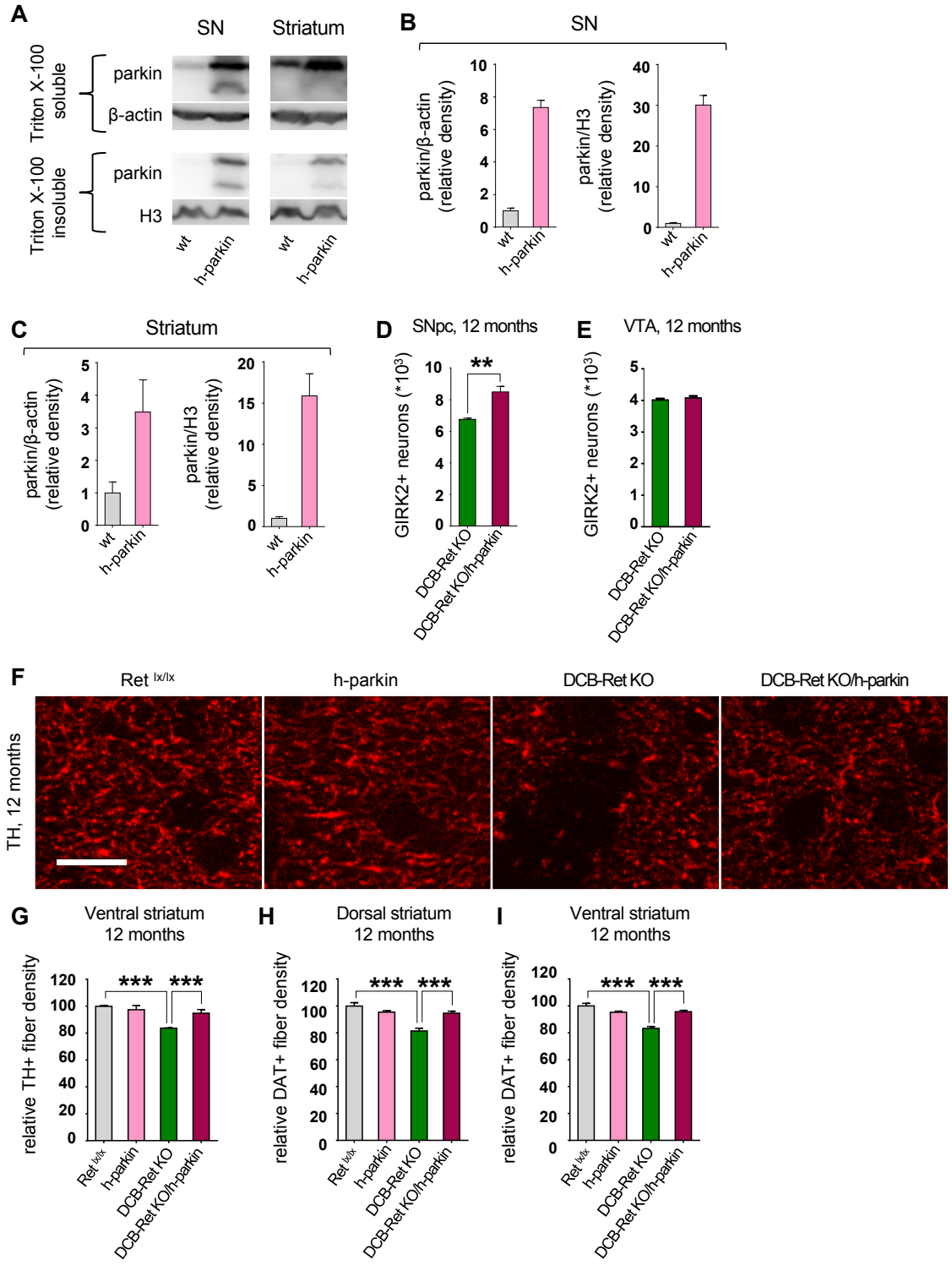

Supplemental Figure 7. Transgenic parkin prevents neurodegeneration in Ret deficient mice. (**A**) Representative Western blot images showing the amount of parkin in Triton X-100-soluble and -insoluble fractions of the SN and striatum protein lysates from adult wt (wildtype) and h-parkin transgenic mice. β-actin and histone H3 were used as loading controls for Triton X-100-soluble and -insoluble fractions, respectively. (**B and C**) Quantifications of Western blots for parkin protein from (B) SN and (C) striatum lysates obtained from 3 or 4 mice per genotype. In some cases, lysates from h-parkin show an extra band below the normal parkin protein band, which originates from an internal translation start site in the human parkin transcript and this isoform lacks the UBL domain (Henn et al., 2005). (**D and E**) Stereological quantifications of the GIRK2 positive neurons in the (D) SNpc and (E) VTA of 12 months old mice of the indicated genotypes (n = 3). (**F**) Representative images of coronal sections from 12 month old mice of the indicated genotypes showing DA fiber innervation in the dorsal striatum immunofluorescently labeled with TH antibody (scale bar: 250 µm). (**G to I**) Quantifications of the TH fiber density in (G) ventral striatum and DAT fiber density in the (H) dorsal and (I) ventral striatum of 12 month old mice of the indicated genotypes (n = 3-5). (data are represented as mean +/- SEM; ** p≤0.01, *** p≤0.001; unpaired two tailed t-test for D and E; One-way ANOVA, Newman-Keuls post-hoc test for G, H and I).

Supplemental Figure 8

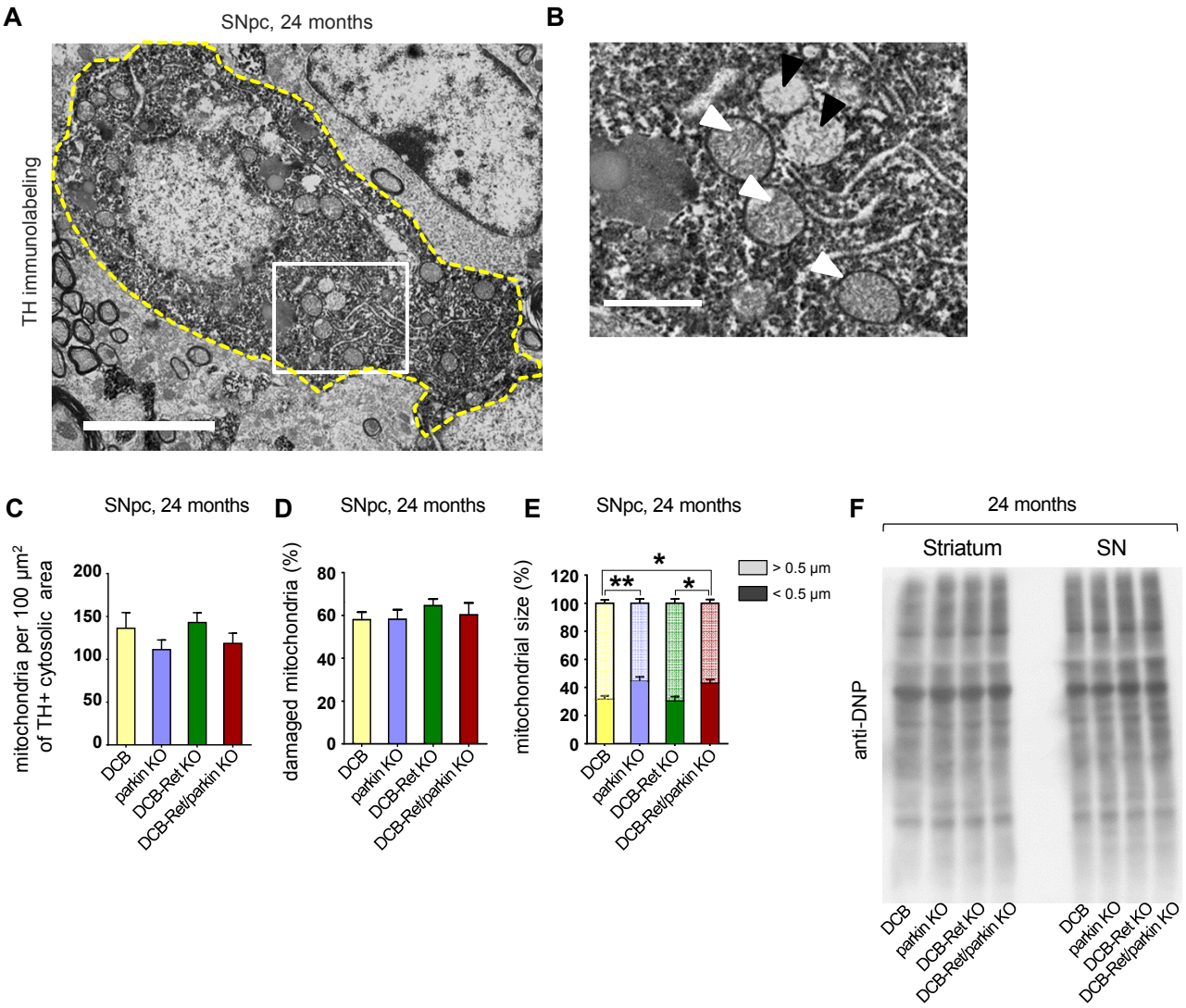

Supplemental Figure 8. Electron microcopy study of mitochondrial morphology in SNpc DA neurons and detection of protein oxidation in the striatum and SN of 24 months old mice. (**A and B**) Representative electron microscopy image of (A) TH immunolabeled DA neuron is surrounded with dotted yellow line (darkly stained due to DAB reaction), from the SNpc of a 24 month old DCB control mouse (scale bar: 5 µm). (B) Enlarged image of the rectangle in A depicting normal (marked with white triangles) and damaged (marked with black triangles) mitochondria (scale bar: 1 µm). (**C to E**) Quantifications of (C) total number of mitochondria per 100 µm^2 TH positive cytosolic area, (D) percentage of damaged mitochondria and (E) percentage of larger mitochondria (> 0.5 µm, shown as light shaded bars) and smaller mitochondria (< 0.5 µm, shown as dark shaded bars) of 24 month old mice of the indicated genotypes (n = 3-4, data are represented as mean +/- SEM; * p≤0.05, ** p≤0.01; One-way ANOVA, Newman-Keuls post-hoc test for C and D; Two-way ANOVA, Newman-Keuls post-hoc test for E). (**F**) Western blot image depicting carbonylated proteins detected by anti-DNP (2,4-dinitrophenylhydrazone) antibody following derivatization of the Striatum and SN protein lysates with DNPH (2,4-dinitrophenylhydrazine) provided in the OxyBlot Protein Oxidation Detection Kit (from Millipore); 24 months old mice of indicated genotypes were used for the assay (the assay was performed on lysates from n = 4 mice per genotype, n = 1 per genotype is shown).

Supplemental Figure 9

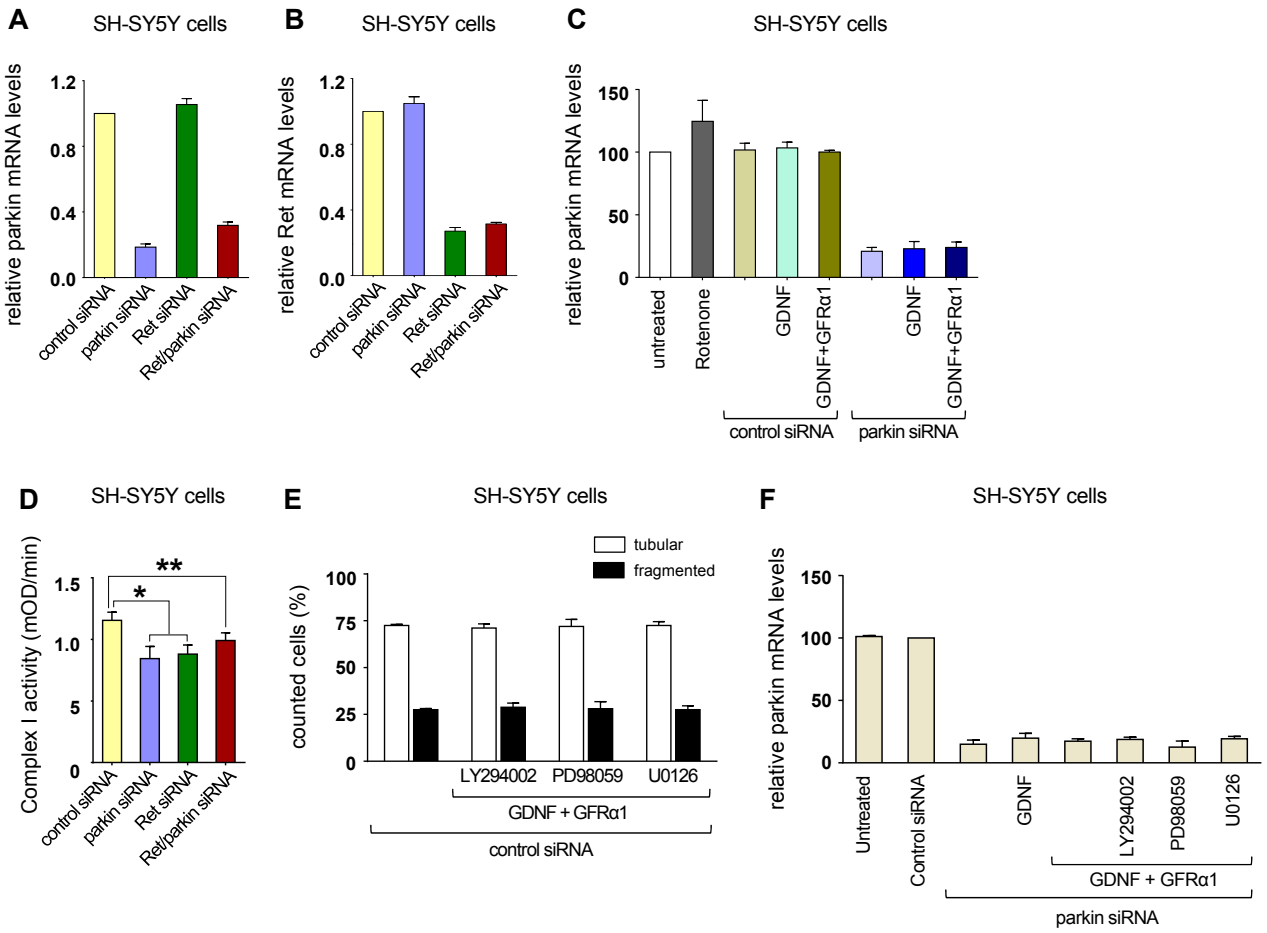

Supplemental Figure 9. Effect of parkin and Ret knockdown on complex I activity, effect of different signaling molecule inhibitors on mitochondrial morphology in SH-SY5Y cells. (**A and B**) Quantification of the relative (A) parkin and (B) Ret mRNA levels in cells treated with control, parkin, Ret or both parkin and Ret siRNAs. These samples were used for measuring total ATP levels in Figure 4E (n = 4 experiments, data are represented as mean +/- SEM). (**C**) Quantification of the relative parkin mRNA levels cells untreated cells, cells treated with Rotenone, with control siRNA or parkin siRNA alone or together with GDNF or GDNF+GFRα1 . These samples were used for measuring total ATP levels in Figure 4G (n = 4 experiments). (**D**) Quantifications of mitochondrial complex I activity in the SH-SY5Y cells treated with control, parkin, Ret or both parkin and Ret siRNA as indicated (n = 5 experiments, data are represented as mean +/- SEM, * p≤0.05, ** p≤0.01, two-tailed, paired t-test). (**E**) Quantification of cells with tubular (white bar) or fragmented (black bar) mitochondria treated with control siRNA alone or control siRNA together with GDNF and GFRα1 along with one of the inhibitors LY294002 (PI3K inhibitor) PD98059 (MEK1 inhibitor) and U0126 (MEK 1+2 inhibitor) (n = 3 experiments, data are represented as mean +/- SEM). (**F**) Quantification of relative parkin mRNA levels in untreated cells, cells treated with control siRNA alone or control siRNA together with GDNF, GDNF+GFRα1 and GDNF+GFRα1 along with one of the inhibitors - LY294002 (PI3K inhibitor), PD98059 (MEK1 inhibitor) or U0126 (MEK 1+2 inhibitor) (n = 3 experiments, data are represented as mean +/- SEM; * p≤0.05, ** p≤0.01; paired two tailed t-test).

Supplemental Figure 10

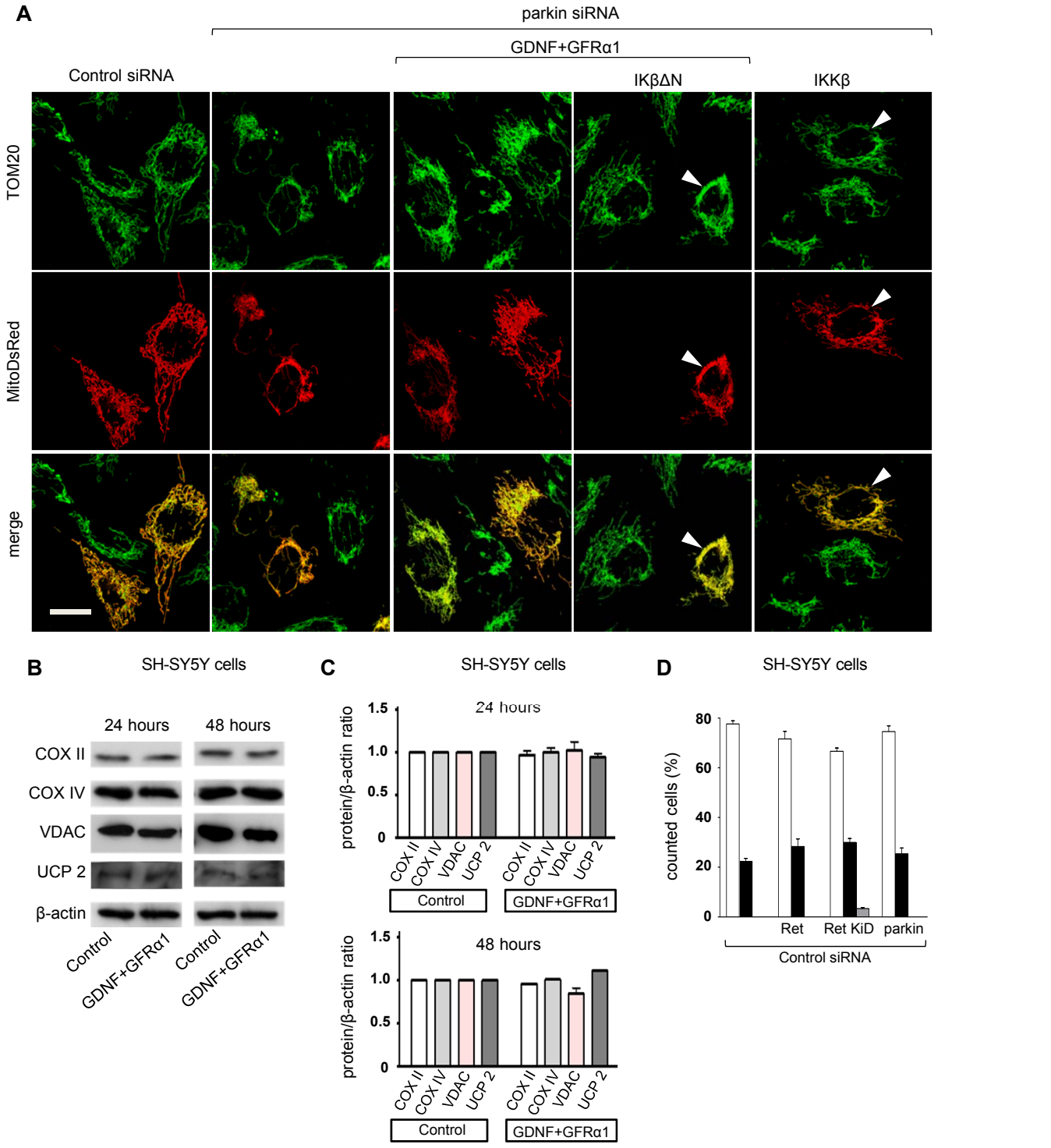

Supplemental Figure 10. GDNF signaling can prevent parkin deficiency induced mitochondrial fragmentation. (**A**) Representative images showing alterations in mitochondrial morphology after transfection with control or parkin siRNA with or without overexpression of IKβΔN or IKKβ and additional treatment with GDNF+GFRα1 as indicated. Mitochondria are stained with TOM20 antibody (green) in the upper row and MitoDsRed used as transfection control shown in (red) in the middle row and overlay (yellow) is shown in the bottom row (scale bar: 10μm). The quantification of this experiment is shown in Figure 5E. (**B and C**) Shown are (B) Western blot images and the (D) densitometrical quantification of the bands of the indicated proteins in cell lysates of GDNF+GFRα1 treated and non-treated (control) SH-SY5Y cells 24 and 48 hour after treatment. β-actin is shown as loading control and to normalize the samples. (**D**) Quantification of SH-SY5Y cells with tubular (white bar), fragmented (black bar) or condensed (gray bar) mitochondria after transfection with control siRNA combined with overexpression of Ret, kinase dead Ret (Ret KiD) or parkin as indicated. (n = 3 experiments, data are represented as mean +/- SEM).

Supplemental Figure 11

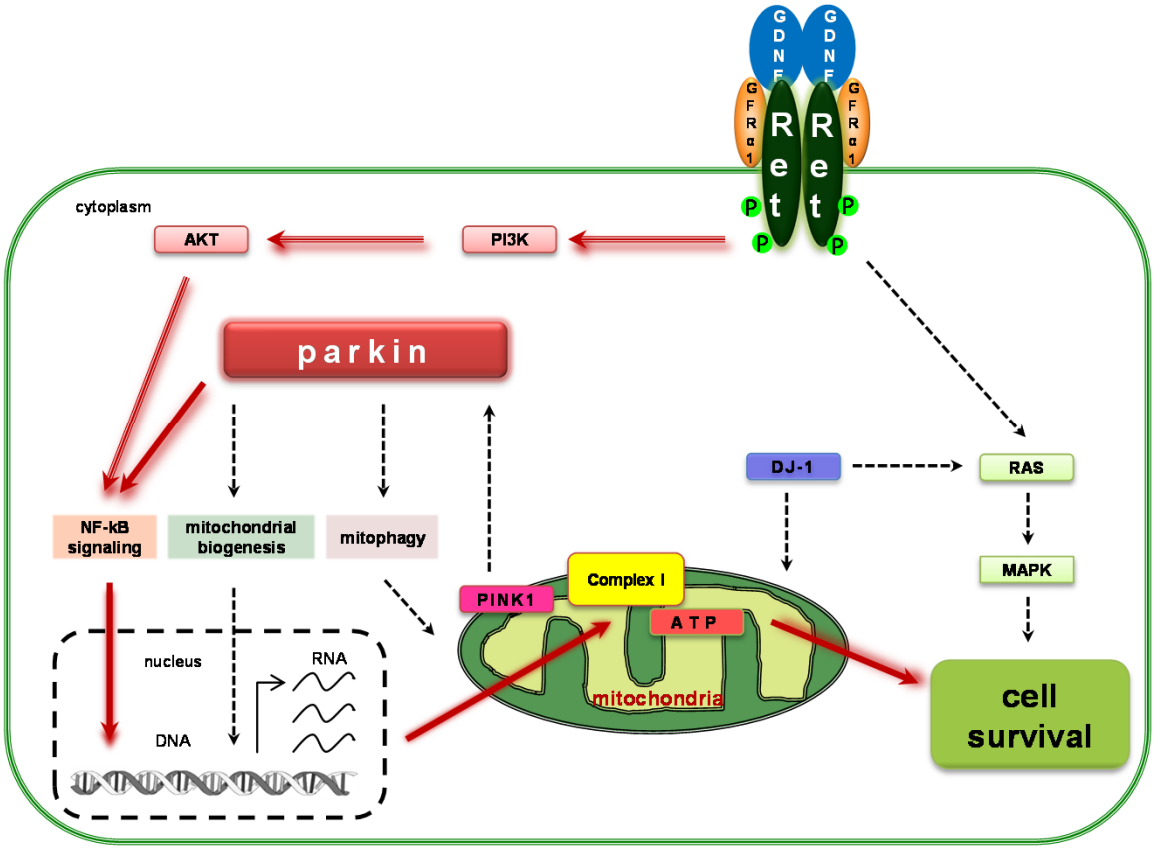

Supplemental Figure 11. Converging signaling cascades of Ret and parkin to ensure mitochondrial integrity and substantia nigra dopaminergic neuron maintenance. Red arrows show the here described activation of the NF-κB pathway through Ret, PI3K and Akt leading to stimulation of ATP synthesis via the mitochondrial complex I and thus promotes cell survival.

Supplemental Table 1

antibody (α-)	company/source	catalog number	Host	clonality	working dilution
Ret	lab made	-	rabbit	monoclonal	1:250
Parkin	AbD serotec	AHP495	goat	polyclonal	1:500
TH	Diasorin	22941	mouse	monoclonal	1:1000
DAT	Chemicon	MAB369	rat	monoclonal	1:500
GIRK2	Almone labs	APC-006	rabbit	polyclonal	1:500
GFAP	DaKO	Z0334	rabbit	polyclonal	1:500
Iba1	WaKO	MNQ4255	rabbit	polyclonal	1:500
TOM20	Santa Cruz Biotechnology	sc-11415	rabbit	polyclonal	1:500

Supplemental Table 1. Antibodies used for immunohistochemistry and immunocytochemistry

Supplemental Table 2

antibody (α-)	company/source	catalog number	host	clonality	working dilution
Ret	lab made	-	rabbit	monoclonal	1:1000
Parkin	Santa Cruz Biotechnology	sc-32282	mouse	monoclonal	1:500
TH	Diasorin	22941	mouse	monoclonal	1:20000
β-actin	Sigma-Aldrich	A2228	mouse	monoclonal	1:20000
phospho-Akt (Ser 473)	Cell Signaling Technology	4051	mouse	monoclonal	1:1000
phospho-S6 (S235/236)	Cell Signaling Technology	4858	rabbit	monoclonal	1:1000
phospho-ERK1/2 (Thr202/Tyr204)	Cell Signaling Technology	4370	rabbit	monoclonal	1:1000
Akt (pan)	Cell Signaling Technology	4691	rabbit	monoclonal	1:1000
S6	Cell Signaling Technology	2317	mouse	monoclonal	1:1000
ERK1/2	Cell Signaling Technology	4695	rabbit	monoclonal	1:1000
DAT	Chemicon	MAB369	rat	monoclonal	1:500
NDUFA10	Santa Cruz Biotechnology	sc-292084	rabbit	polyclonal	1:1000
Histone 3 (H3)	Cell Signaling Technology	9715	rabbit	monoclonal	1:1000
Opa1	BD Transduction Laboratories	612607	mouse	monoclonal	1:1000
Drp1	BD Transduction Laboratories	611112	mouse	monoclonal	1:1000
Mfn1	Abcam	ab57602	mouse	monoclonal	1:1000
Mfn2	Sigma-Aldrich	M6319	rabbit	monoclonal	1:1000
COXII	Epitomics	AC-0273	rabbit	monoclonal	1:1000
COXIV	Cell Signaling Technology	4844	rabbit	polyclonal	1:500
VDAC	Calbiochem	MABN504	mouse	monoclonal	1:1000
UCP-2	Santa Cruz Biotechnology	sc-6526	goat	polyclonal	1:1000
p62	Enzo Life Sciences	BML-PW9860	rabbit	polyclonal	1:1000
LC3	Novus Biologicals	NB100-2220	rabbit	polyclonal	1:2000
GDNF	R & D Systems	AF212NA	goat	polyclonal	1:500
GFRα1	Santa Cruz Biotechnology	sc-10716	rabbit	polyclonal	1:500
GFRα2	Santa Cruz Biotechnology	sc-7136	goat	polyclonal	1:500
α-synuclein	Santa Cruz Biotechnology	sc-69977	mouse	monoclonal	1:500
α-tubulin	Sigma-Aldrich	T-9026	mouse	monoclonal	1:20000
DNP	Millipore	90451	rabbit	polyclonal	1:150

Supplemental Table 2. Antibodies used for Western blotting

Within each column, compare rows (simple effects within columns)							p not significant = n.s		
							p < 0,05 *		
Number of families	3						p < 0,01**		
Number of comparisons per family	10						p < 0,001 ***		
Alpha	0,05						p < 0,0001 ****		
Newman-Keuls multiple comparisons test		Tubular			Fragmented			Condensed	
	Mean Diff,	Significant?	Summary	Mean Diff,	Significant?	Summary	Mean Diff,	Significant?	Summary
Ret siRNA vs. control siRNA	-53,37	Yes	****	31,67	Yes	****	21,7	Yes	****
Ret siRNA+Ret vs. control siRNA	-10,3	Yes	**	7,633	Yes	*	2,67	No	ns
Ret siRNA+Ret KiD vs. control siRNA	-50,43	Yes	****	25,97	Yes	****	24,46	Yes	****
Ret siRNA+parkin vs. control siRNA	-8,013	Yes	**	4,733	No	ns	3,28	No	ns
Ret siRNA+Ret vs. Ret siRNA	43,06	Yes	****	-24,03	Yes	****	-19,03	Yes	****
Ret siRNA+Ret KiD vs. Ret siRNA	2,933	No	ns	-5,693	Yes	*	2,76	No	ns
Ret siRNA+parkin vs. Ret siRNA	45,35	Yes	****	-26,93	Yes	****	-18,42	Yes	****
Ret siRNA+Ret KiD vs. Ret siRNA+Ret	-40,13	Yes	****	18,34	Yes	****	21,79	Yes	****
Ret siRNA+parkin vs. Ret siRNA+Ret	2,29	No	ns	-2,9	No	ns	0,61	No	ns
Ret siRNA+parkin vs. Ret siRNA+Ret KiD	42,42	Yes	****	-21,24	Yes	****	-21,18	Yes	****

Supplemental Table 3. Newman-Keuls multiple comparison test performed post Two-way ANOVA analysis for the data in Figure 7C

Within each column, compare rows (simple effects within columns)						p not significant = n.s			
Number of families	3					p < 0,05 *			
Number of comparisons per family	45					p < 0,01**			
Alpha	0,05					p < 0,001 ***			
						p < 0,0001 ****			
		Tubular			Fragmented			Condensed	
Newman-Keuls multiple comparisons test	Mean Diff,	Significant?	Summary	Mean Diff,	Significant?	Summary	Mean Diff,	Significant?	Summary
control siRNA vs. IKBdN	10,84	Yes	***	-10,84	Yes	**	0	No	ns
control siRNA vs. Ret siRNA	50	Yes	****	-23,93	Yes	****	-26,07	Yes	****
control siRNA vs. Ret siRNA+IKBdN	52,02	Yes	****	-23,02	Yes	****	-29	Yes	****
control siRNA vs. Ret siRNA+PI3Kwt	27,15	Yes	****	-12,05	Yes	***	-15,1	Yes	****
control siRNA vs. Ret siRNA+PI3Kwt+IKBdN	42,39	Yes	****	-23,75	Yes	****	-18,63	Yes	****
control siRNA vs. Ret siRNA +PI3Kmyr	10,95	Yes	***	-0,2527	No	ns	-10,7	Yes	***
control siRNA vs. Ret siRNA+PI3Kmyr+GDNF+GFRa1	9,726	Yes	***	1,281	No	ns	-11,01	Yes	***
control siRNA vs. Ret siRNA+Men2A	29,43	Yes	****	-10,55	Yes	**	-18,88	Yes	****
control siRNA vs. Ret siRNA+Men2A+GDNF+GFRa1	22,62	Yes	****	-7,769	Yes	*	-14,85	Yes	****
IKBdN vs. Ret siRNA	39,15	Yes	****	-13,09	Yes	****	-26,07	Yes	****
IKBdN vs. Ret siRNA+IKBdN	41,18	Yes	****	-12,18	Yes	****	-29	Yes	****
IKBdN vs. Ret siRNA+PI3Kwt	16,31	Yes	****	-1,21	No	ns	-15,1	Yes	****
IKBdN vs. Ret siRNA+PI3Kwt+IKBdN	31,54	Yes	****	-12,91	Yes	****	-18,63	Yes	****
IKBdN vs. Ret siRNA +PI3Kmyr	0,11	No	ns	10,59	Yes	**	-10,7	Yes	***
IKBdN vs. Ret siRNA+PI3Kmyr+GDNF+GFRa1	-1,117	No	ns	12,12	Yes	***	-11,01	Yes	***
IKBdN vs. Ret siRNA+Men2A	18,59	Yes	****	0,29	No	ns	-18,88	Yes	****
IKBdN vs. Ret siRNA+Men2A+GDNF+GFRa1	11,78	Yes	***	3,073	No	ns	-14,85	Yes	****
Ret siRNA vs. Ret siRNA+IKBdN	2,027	No	ns	0,91	No	ns	-2,937	No	ns
Ret siRNA vs. Ret siRNA+PI3Kwt	-22,84	Yes	****	11,88	Yes	***	10,97	Yes	***
Ret siRNA vs. Ret siRNA+PI3Kwt+IKBdN	-7,61	Yes	**	0,1767	No	ns	7,433	Yes	*
Ret siRNA vs. Ret siRNA +PI3Kmyr	-39,04	Yes	****	23,68	Yes	****	15,37	Yes	****
Ret siRNA vs. Ret siRNA+PI3Kmyr+GDNF+GFRa1	-40,27	Yes	****	25,21	Yes	****	15,06	Yes	****
Ret siRNA vs. Ret siRNA+Men2A	-20,56	Yes	****	13,38	Yes	****	7,187	Yes	**
Ret siRNA vs. Ret siRNA+Men2A+GDNF+GFRa1	-27,38	Yes	****	16,16	Yes	****	11,22	Yes	***
Ret siRNA+IKBdN vs. Ret siRNA+PI3Kwt	-24,87	Yes	****	10,97	Yes	***	13,9	Yes	****
Ret siRNA+IKBdN vs. Ret siRNA+PI3Kwt+IKBdN	-9,637	Yes	**	-0,7333	No	ns	10,37	Yes	**
Ret siRNA+IKBdN vs. Ret siRNA +PI3Kmyr	-41,07	Yes	****	22,77	Yes	****	18,3	Yes	****
Ret siRNA+IKBdN vs. Ret siRNA+PI3Kmyr+GDNF+GFRa1	-42,3	Yes	****	24,3	Yes	****	18	Yes	****
Ret siRNA+IKBdN vs. Ret siRNA+Men2A	-22,59	Yes	****	12,47	Yes	****	10,12	Yes	***
Ret siRNA+IKBdN vs. Ret siRNA+Men2A+GDNF+GFRa1	-29,4	Yes	****	15,25	Yes	****	14,15	Yes	****
Ret siRNA+PI3Kwt vs. Ret siRNA+PI3Kwt+IKBdN	15,23	Yes	****	-11,7	Yes	***	-3,533	No	ns
Ret siRNA+PI3Kwt vs. Ret siRNA +PI3Kmyr	-16,2	Yes	****	11,8	Yes	***	4,4	No	ns
Ret siRNA+PI3Kwt vs. Ret siRNA+PI3Kmyr+GDNF+GFRa1	-17,43	Yes	****	13,33	Yes	***	4,093	No	ns
Ret siRNA+PI3Kwt vs. Ret siRNA+Men2A	2,28	No	ns	1,5	No	ns	-3,78	No	ns
Ret siRNA+PI3Kwt vs. Ret siRNA+Men2A+GDNF+GFRa1	-4,533	No	ns	4,283	No	ns	0,25	No	ns
Ret siRNA+PI3Kwt+IKBdN vs. Ret siRNA +PI3Kmyr	-31,43	Yes	****	23,5	Yes	****	7,933	Yes	*
Ret siRNA+PI3Kwt+IKBdN vs. Ret siRNA+PI3Kmyr+GDNF+GFRa1	-32,66	Yes	****	25,03	Yes	****	7,627	Yes	*
Ret siRNA+PI3Kwt+IKBdN vs. Ret siRNA+Men2A	-12,95	Yes	****	13,2	Yes	****	-0,2467	No	ns
Ret siRNA+PI3Kwt+IKBdN vs. Ret siRNA+Men2A+GDNF+GFRa1	-19,77	Yes	****	15,98	Yes	****	3,783	No	ns
Ret siRNA +PI3Kmyr vs. Ret siRNA+PI3Kmyr+GDNF+GFRa1	-1,227	No	ns	1,533	No	ns	-0,3067	No	ns
Ret siRNA +PI3Kmyr vs. Ret siRNA+Men2A	18,48	Yes	****	-10,3	Yes	***	-8,18	Yes	*
Ret siRNA +PI3Kmyr vs. Ret siRNA+Men2A+GDNF+GFRa1	11,67	Yes	****	-7,517	Yes	**	-4,15	No	ns
Ret siRNA+PI3Kmyr+GDNF+GFRa1 vs. Ret siRNA+Men2A	19,71	Yes	****	-11,83	Yes	***	-7,873	Yes	*
Ret siRNA+PI3Kmyr+GDNF+GFRa1 vs. Ret siRNA+Men2A+GDNF+GFRa1	12,89	Yes	****	-9,05	Yes	**	-3,843	No	ns
Ret siRNA+Men2A vs. Ret siRNA+Men2A+GDNF+GFRa1	-6,813	Yes	*	2,783	No	ns	4,03	No	ns

Supplemental Table 4. Newman-Keuls multiple comparison test performed post Two-way ANOVA analysis for the data in Figure 7E